ELSEVIER

Chemical Engineering Journal 111 (2005) 91–103

Chemical Engineering Journal

www.elsevier.com/locate/cej

Numerical identification of parameters for a flocculated suspension from concentration measurements during batch centrifugation

S. Berres [a], R. Bürger [b], A. Coronel [b,c], M. Sepúlveda [b,*]

[a] *Institut für Angewandte Analysis und Numerische Simulation, Universitat Stuttgart, Pfaffenwaldring 57, D-70569 Stuttgart, Germany*
[b] *Departamento de Ingeniería Matemática, Universidad de Concepción, Casilla 160-C, Concepción, Chile*
[c] *Departamento de Ciencias Básicas, Facultad de Ciencias, Universidad del Bío-Bío, Casilla 447, Campus Fernando May, Chilián, Chile*

Abstract

This paper presents a new mathematical technique for the identification of two rheological model functions (namely, the hindered settling and effective solid stress functions) obtained from concentration profiles measured during the centrifugation of flocculated suspensions. We consider both a rotating tube and a basket centrifuge at a given angular velocity, and assume that the radius (i.e., the distance to the center of rotation) is the only spatial coordinate. The governing equation is a non-standard strongly degenerate parabolic partial differential equation for the solids volume fraction as a function of radius and time whose coefficients involve the model functions. We present a numerical technique for the parameter identification problem suitable for this type of equations, and apply it to determine the model functions in two numerical examples.

Keywords: Flocculated suspensions; Parameter identification; Centrifugation; Numerical technique

1. Introduction

Solid–liquid separation or dewatering processes of flocculated suspensions, including the unit operations of thickening, clarification, centrifugation and filtration, can be modeled by a recent theory of sedimentation-consolidation processes developed in [1–3]. This theory is equivalent to the theory of suspension dewatering utilized in [4–7] (see also the references cited in these works). Whenever the process considered admits a spatially one-dimensional description, the sedimentation-consolidation model reduces to a second-order parabolic scalar partial differential equation for the local solids volume fraction ϕ as a function of the spatial coordinate and time. The coefficients of this governing equation involve two material specific model functions characterizing the suspension under study, the hindered settling or Kynch batch flux density function $f_{bk}(\phi)$ and the effective solid stress function $\sigma_e(\phi)$. A particular feature of the governing equation lies in the absence of effective solid stress whenever the particles are in hindered settling, that is, whenever their volume fraction ϕ does not exceed a critical concentration or gel point ϕ_c. In this case, the sedimentation-consolidation equation degenerates into the first-order conservation law of Kynch's well-known kinematic sedimentation theory [8,9], which was extended to the centrifugation of suspensions in [10,11]. The unusual type-change feature of the governing partial differential equation made a deep mathematical analysis of degenerate parabolic equations necessary (see, for example, [12–15]). The benefits of this research for the engineering community are reliable numerical methods for the simulation of solid-liquid separation processes [16,17]. Numerous comparisons with experimental data [18,19] confirmed that the sedimentation-consolidation model indeed is a useful tool for the simulation, control and design of solid–liquid separation processes [20,21].

In spite of all these advances, one mandatory prerequisite for the application of the sedimentation-consolidation theory, namely the necessity to determine the functions $f_{bk}(\phi)$ and $\sigma_e(\phi)$ by experimentation, has persisted. Recent reports of experimental techniques aiming at determining these or equivalent material specific model functions by settling, fil-

* Corresponding author.
E-mail addresses: berres@mathematik.uni-stuttgart.de (S. Berres), buerger@mathematik.uni-stuttgart.de (R. Bürger), acoronel@roble.fdo-may.ubiobio.cl (A. Coronel), mauricio@ing-mat.udec.cl (M. Sepúlveda).

1385-8947/$ – see front matter © 2005 Elsevier B.V. All rights reserved.
doi:10.1016/j.cej.2005.02.005

tration, and centrifugation include [22–32,5,7], respectively. The present paper, as our previous studies [33,34], presents an accurate and automatic mathematical technique to extract the desired model functions from concentration measurements that could, for example, have been obtained from computerized axial tomographic scanner (CATSCAN) measurements (as in [22–25]) or by light extinction profiles [27].

To outline the scope of this paper, we recall that the mathematical model describing the centrifugation process is given by a second-order degenerate parabolic partial differential equation (PDE), whose coefficients are determined by the functions $f_{bk}(\phi)$ and $\sigma_e(\phi)$. In our case, these functions are unknown, and concentration measurements, so-called observations, either at fixed times or at fixed radial positions are available. We interpret these measurements as part of a solution to the PDE, and seek to determine the coefficient functions in such a way that the error between the observation and the solution of the PDE is minimized. Interpreting this error as a cost functional, we see that the task of parameter identification essentially is an *optimization problem*.

The problem of calculating back the coefficients of a PDE from a given solution is usually referred to as a *parameter identification problem*. The slightly more general mathematical area of *inverse problems* also includes, for example, the reconstruction of initial conditions for a given solution. A large number of authors proposed analytical and numerical methods for inverse problems in evolution partial differential equations, see for example [35–42] and the references cited in these papers. The basic difficulty is that inverse problems are highly ill-posed, which implies non-uniqueness in most situations. In fact, different initial conditions or coefficient functions may lead to the same solution, which means that the optimization problem is likely not to be uniquely solvable due to several local minima of the cost functional. This property requires that the final result of the parameter identification procedure be verified and, for example, compared with findings for similar materials with known parameters, before it can be accepted for further simulation, control, design and related scale-up calculations.

The governing equation of the centrifugation model is a non-linear second-order parabolic equation which degenerates to first-order hyperbolic type, where the location of type change is unknown a priori and therefore, part of the solution of the problem. For gravity settling in a column, a similar numerical parameter identification technique, was presented recently by Coronel et al. [34].

The remainder of the paper is organized as follows. In Section 2, we adopt a spatially one-dimensional model for centrifugation of flocculated suspensions that is described in detail in [43], and which is a special case of a spatially multidimensional mathematical framework for these mixtures provided by [3]. This model appears in two variants for rotating tubes and basket centrifuges, respectively. In both cases, the resulting mathematical model is an initial-boundary value problem for a strongly degenerate quasilinear parabolic partial differential equation for $\phi = \phi(r, t)$. We emphasize that the discussion is limited to two particular parametric forms of the functions $f_{bk}(\phi)$ and $\sigma_e(\phi)$. This makes the parameter identification problem tractable, since instead of attempting to determine these functions as a whole, we only need to find four scalar real constants appearing in particular semi-empiricial power-law type approaches for these functions.

In Section 3 we provide the mathematical framework of the parameter identification problem. The parameters of the constitutive functions, which are collected in the common parameter vector e, depend on the material properties of the suspension considered. Our goal is to determine **e**. To this end, for any given parameter vector **e**, we denote by $\phi(\mathbf{e})$ the solution of the initial-boundary value problem describing the centrifugation process, and denote by $\mathcal{J}(\phi)$ the functional measuring the error, that is, the distance to the observation. The solution property of ϕ is expressed in the weak form "$E(\phi, p; \mathbf{e}) = 0$ for all test functions p". We replace the unconstrained minimization problem "minimize $\mathcal{J}(\phi(\mathbf{e}))$" by the minimization problem "minimize $\mathcal{L}(\phi, p; \mathbf{e}) := \mathcal{J}(\phi) - E(\phi, p; \mathbf{e})$", where $\mathcal{L}$ is the Lagrangian of the constrained minimization problem "minimize $\mathcal{J}(\phi)$ under the side condition $E(\phi, p, \mathbf{e}) = 0$". To solve this minimization problem, we need to determine the test function p, which acts as a Lagrangian multiplier, in such a way that $\partial\mathcal{L}/\partial\phi = 0$ vanishes. This problem is called the adjoint problem. Its solution permits to calculate the gradient of the cost function $\mathcal{J}$ with respect to **e**. This gradient leads to an improved choice of **e**. The existence of solutions for the inverse problem is a consequence of the continuous dependence of the entropy solutions on the flux and the diffusion for a degenerate parabolic equation (see [33,34,44,45]). However, we cannot expect this solution to be unique.

The formal calculus of Section 3 cannot be performed exactly. To apply it to solve real-world problems, we need to transfer it to a discrete version, which is derived in Section 4. One step in this procedure is the solution of the forward or direct problem. For its discretization, we consider a finite volume scheme in conservative form with an Engquist–Osher approximation for the numerical flux [17,43,46]. The result is an optimization scheme for identification. (Some technical details are deferred to Appendix A) In Section 5 we present some numerical examples of parameter identification for this problem. Finally, Section 6 collects conclusions and some final remarks due in light of the analysis and numerical results.

2. The centrifugation model

Fig. 1 shows the two configurations considered: (a) a tube and (b) a basket centrifuge, both rotating at a given angular velocity ω. To distinguish between these cases, we introduce a parameter σ taking the values $\sigma = 0$ and $\sigma = 1$ in the former and latter case, respectively. The unique spatial coordinate is the radius r, which varies between an inner radius $R_0 > 0$ and an outer radius $R > R_0$, corresponding to the suspension meniscus and the outer wall, respectively. It should be em-

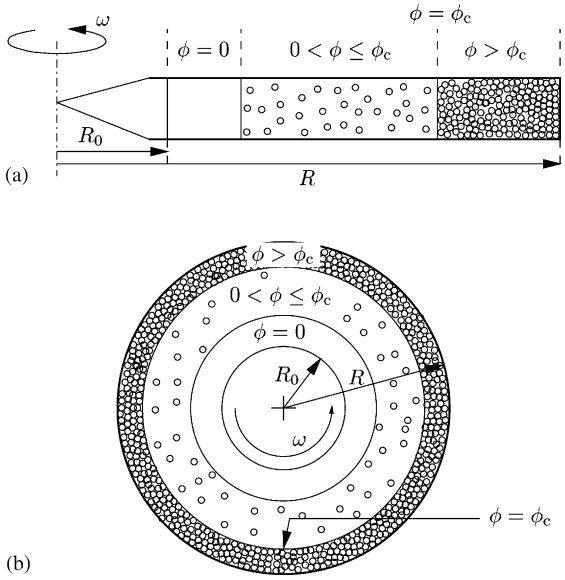

Fig. 1. (a) Rotating tube with constant cross-section ($\sigma = 0$), (b) rotating axisymmetric cylinder ($\sigma = 1$). The concentration zones are the clear liquid ($\phi = 0$), the hindered settling zone ($0 < \phi \le \phi_c$) and the compression zone $\phi > \phi_c$.

phasized that the reduction to one space dimension represents a strong simplification that is acceptable under several restrictions only. In particular, the angular velocity ω must be large enough such that the centrifugal body force is dominant and the gravitational can be neglected, but on the other hand not so large that Coriolis effects would become important. Moreover, the effect of sedimentation onto the side walls of tubular centrifuges (case $\sigma = 0$) is neglected. The limitations of such one-dimensional models, which were first introduced by Anestis and Schneider [10,11] (see also [47]), are clearly discussed by Ungarish [48]. However, the alternative of passing to several space dimensions in the framework of the phenomenological model would mean that additional equations for the motion of the mixture would have to be solved. We assume here the viewpoint that the conditions allowing for the above-mentioned simplification are satisfied. This view is supported by a series of recently published centrifugation experiments [29,32], which exhibit good agreement with the predictions of one-dimensional models.

The resulting strongly degenerate quasilinear parabolic partial differential equation is

$$\frac{\partial \phi}{\partial t} + \frac{1}{r^\sigma}\frac{\partial}{\partial r}\left(-\frac{\omega^2}{g} r^{1+\sigma} f_{\mathrm{bk}}(\phi)\right) = \frac{1}{r^\sigma}\frac{\partial}{\partial r}\left(r^\sigma \frac{\partial A(\phi)}{\partial r}\right), \quad (r,t) \in Q_T := (R_0, R) \times (0, T), \tag{2.1}$$

where g is the acceleration of gravity, R_0 the radius of the inner suspension meniscus and R that of the outer wall. The functions $f_{\mathrm{bk}}(\phi)$ and $A(\phi)$ are the Kynch batch flux density function and the integrated diffusion coefficient, respectively, which describe the rheology of the suspension under consideration. These functions account for hindered settling and sediment compressibility, respectively. For simplicity, we assume that $f_{\mathrm{bk}}(\phi)$ is a continuous and piecewise differentiable function satisfying $f_{\mathrm{bk}}(\phi) = 0$ for $\phi \le 0$ and $\phi \ge \phi_{\max}$, where $\phi_{\max}$ is the maximum solids concentration, and $f_{\mathrm{bk}}(\phi) < 0$ for $0 < \phi < \phi_{\max}$. The function $A(\phi)$ is the primitive of the diffusion coefficient $a(\phi)$,

$$A(\phi) = \int_0^\phi a(s)\,\mathrm{d}s,$$

where $a(\phi)$ is given by

$$a(\phi) := -\frac{f_{\mathrm{bk}}(\phi)\sigma_{\mathrm{e}}'(\phi)}{\Delta\varrho g \phi}.$$

Here, $\Delta\varrho$ is the solid–fluid density difference, and $\sigma_{\mathrm{e}}'(\phi)$ is the derivative of effective solid stress function $\sigma_{\mathrm{e}}(\phi)$. The function $\sigma_{\mathrm{e}}(\phi)$ is assumed to vanish as long as the solid flocs are in hindered settling and not in contact, which occurs wherever ϕ does not exceed a critical concentration ϕ_c, and to be a strictly increasing function of ϕ for $\phi > \phi_c$, i.e., we have

$$\sigma_{\mathrm{e}}(\phi) \begin{cases} = 0 & \text{for } \phi \le \phi_c, \\ > 0 & \text{for } \phi > \phi_c, \end{cases} \qquad \sigma_{\mathrm{e}}'(\phi) \begin{cases} = 0 & \text{for } \phi \le \phi_c, \\ > 0 & \text{for } \phi > \phi_c. \end{cases}$$

Combining the assumptions on f_{bk} and on σ_{e}, we see that

$$a(\phi) \begin{cases} = 0 & \text{for } \phi \le \phi_c \text{ and } \phi \ge \phi_{\max}, \\ > 0 & \text{for } \phi_c < \phi < \phi_{\max}. \end{cases}$$

Thus, (2.1) is a first-order hyperbolic partial differential equation for $\phi \le \phi_c$ and $\phi \ge \phi_{\max}$ and a second-order parabolic partial differential equation for $\phi_c < \phi < \phi_{\max}$. Since the degeneracy to hyperbolic type takes place on an interval of solution values of positive length, (2.1) is called *strongly degenerate parabolic*.

In this work, we limit ourselves to two common parametric forms of the model functions f_{bk} and σ_{e}. We assume that according to Richardson and Zaki [49], f_{bk} is given by:

$$f_{\mathrm{bk}}(\phi) \begin{cases} u_\infty \phi (1-\phi)^C & \text{for } 0 < \phi < \phi_{\max}, \\ 0 & \text{for } \phi \le 0 \text{ and } \phi \ge \phi_{\max}, \end{cases} \qquad u_\infty < 0, \quad C \ge 1, \tag{2.2}$$

while the function σ_{e} is defined by the power-law function [50]

$$\sigma_{\mathrm{e}}(\phi) \begin{cases} 0 & \text{for } \phi \le \phi_c, \\ \sigma_0((\phi/\phi_c)^k - 1) & \text{for } \phi > \phi_c, \end{cases} \qquad \sigma_0 > 0, \quad k \ge 1. \tag{2.3}$$

We assume here that u_∞ is a known constant. Thus, if we utilize (2.2) and (2.3), the problem of determining suitable model functions $f_{\mathrm{bk}}(\phi)$ and $\sigma_{\mathrm{e}}(\phi)$ from observations reduces to that of identifying the parameter vector $\mathbf{e} = (C, \phi_c, \sigma_0, k)^{\mathrm{T}}$.

The complete model for the centrifugation of a suspension of an initial concentration $\phi_0 = \phi_0(r)$ is given by (2.1) together

with the initial condition

$$\phi(r,0)=\phi_0(r),\quad r\in[R_0,R], \tag{2.4}$$

where we assume $\phi_0(r)\in[0,\phi_{\max}]$ for $r\in[R_0,R]$, and the kinematic boundary conditions

$$\left(\frac{\omega^2 r_b}{g}f_{bk}(\phi)+\frac{\partial A(\phi)}{\partial r}\right)(r_b,t)=0,\qquad t>0,\quad r_b\in\{R_0,R\}, \tag{2.5}$$

which express that the flux through $r=R_0$ and $r=R$ is zero.

It is well known that solutions of the initial-boundary value problem (2.1), (2.4), (2.5) develop discontinuities due to both the non-linearity of the flux and the degenerate diffusion term, and have to be characterized as weak solutions. To ensure uniqueness, a selection criterion or entropy condition has to be stated to select the physically relevant one among several weak solutions. The precise statement of the solution concept, i.e., the sense in which we understand a *discontinuous* function to be solution to the initial-boundary value problem, requires mathematical preliminaries that are beyond the scope of this contribution and is therefore omitted here; see [33] for details. The proof of existence and uniqueness of an entropy solution of the direct problem is outlined in [13].

Simulations of centrifugation processes obtained by numerical solution of the governing equation (2.1) along with (2.4) and (2.5) are presented in a series of previous papers [13,33,43,51–53], and will not be repeated here. Exact solutions for the special case of an ideal suspension with $A\equiv 0$ are determined by the method of characteristics in [10,11] (see also [47]). Finally, we mention that the model (2.1)–(2.5) has recently been extended to polydisperse suspensions forming compressible sediments [54].

For a suspension forming a compressible sediment, i.e., whenever $A\not\equiv 0$, our model predicts the formation of two moving interfaces, the suspension–supernate interface moving towards the outer radius, and the suspension–sediment interface, at which the concentration exceeds the critical concentration ϕ_c, rising from the outer wall. The former is a curved shock that merges with the sediment–suspension interface after a finite time that is usually referred to as critical time. Furthermore, the concentration of the suspension located between these two interfaces is not constant (as in the gravity case), but decreases as a function of time. The system usually quickly attains a steady-state sediment profile.

3. Mathematical formulation of the parameter identification problem

3.1. The inverse problem as an optimization problem with PDE constraint

The observation data are called $\hat\phi(r,t)$, and may consist of concentration profiles as a function of r, each corresponding to one or several fixed times t, or of concentrations measured at a fixed radius r. To formalize the possible choice of observations, we assume that $\hat\phi(r,t)$ is piecewise constant on rectangles of size $\Delta\hat r\times\Delta\hat t$. Thus, the observation data is given on a structured grid $\hat Q$ with

$$\hat Q:=\{r_1,\dots,r_{\hat J}\}\times\{t_1,\dots,t_{\hat N}\}\subset\bar Q_T:=[R_0,R]\times[0,T].$$

The aim is to determine the parameter vector $\mathbf{e}$ for which the solution of the model problem, $\phi(r,t)$, approximates best the observed data $\hat\phi(r,t)$ (in a sense yet to be described). That solution $\phi=\phi(\mathbf{e})$ depends on the chosen parameters since the constitutive functions $f=f(\mathbf{e})$ and $A=A(\mathbf{e})$ do. This universal dependence of both the solution and the constitutive functions on the parameters will be suppressed for notational convenience.

The parameter identification problem can be written as a constrained optimization problem, where the constraint is given by the direct initial-boundary value problem (2.1), (2.4), (2.5) in its appropriate weak formulation. Thus, the optimization problem can be written as "minimize $\mathcal{J}(\phi)$ under the constraint $\phi=\phi(\mathbf{e})$", where the 'cost function' $\mathcal{J}=\mathcal{J}(\phi)$ measures the quality of approximation. That cost function depends on the parameter vector $\mathbf{e}$ mediated by the model solution. A natural choice is the integrated squared distance between the observed data $\hat\phi$ and the solution $\phi=\phi(\mathbf{e})$ of the model function, which gives rise to the cost function

$$\mathcal{J}(\phi(\mathbf{e})):=\frac{1}{2}\int_{Q_T}(\phi(r,t)-\hat\phi(r,t))^2\delta_{\hat Q}(r,t)\,\mathrm{d}t\,\mathrm{d}r, \tag{3.1}$$

where $\delta_{\hat Q}(r,t)=1$ if $(r,t)\in\hat Q$ and $\delta_{\hat Q}(r,t)=0$ elsewhere. Since first-order equations generally have discontinuous solutions, the governing Eq. (2.1) as constraint on $\phi=\phi(\mathbf{e})$ is replaced by its weak form

$$\begin{aligned}E(\phi,p;\mathbf{e})&:=-\iint_{Q_T}\left\{\phi\frac{\partial p}{\partial t}+f(\phi,r)\frac{\partial p}{\partial r}+A(\phi)\frac{\partial^2 p}{\partial r^2}+s(\phi,r)p\right\}\mathrm{d}t\,\mathrm{d}r+\int_{R_0}^{R}\phi p|_{t=0}^{T}\,\mathrm{d}r\\&\quad+\int_0^T A(\phi)\left(\frac{\partial p}{\partial r}-\sigma\frac{p}{r}\right)\Big|_{r=R_0}^{R}\mathrm{d}t=0,\end{aligned} \tag{3.2}$$

where

$$f(\phi,r):=-\frac{\omega^2 r}{g}f_{bk}(\phi)-\frac{\sigma}{r}A(\phi),$$

$$s(\phi,r):=g\left[\frac{\omega^2}{g}f_{bk}(\phi)+\frac{A(\phi)}{r^2}\right],$$

and p is a test function. Summarizing, we have formulated the parameter identification problem, where a parametrization of the model equations for a given observation is sought, as an optimization problem, where the deviation of the model solution (which has to satisfy the model equations as constraint) from the observations is minimized with respect to the set of all parameters.

3.2. Lagrangian formulation

In classical optimization, it is a common technique to reformulate the optimization problem by adding (or subtracting) the constraint to the cost function. Thus, we consider the following Lagrangian for the problem "minimize $\mathcal{J}(\phi(\mathbf{e}))$ with respect to $\mathbf{e}$"

$$\mathcal{L}(\phi,\, p;\mathbf{e}) := \mathcal{J}(\phi) - E(\phi,\, p;\mathbf{e}). \tag{3.3}$$

The test function p appears here as a generalized Lagrange multiplier related to the constraint $\phi = \phi(\mathbf{e})$. Furthermore, since $E(\phi(\mathbf{e}),\, p;\, \mathbf{e}) = 0$, we have that

$$\mathcal{L}(\phi(\mathbf{e}),\, p;\mathbf{e}) = \mathcal{J}(\phi(\mathbf{e})).$$

In the current application, the cost function is not parametrized by the parameters but only depends on the parameters via the solution of the constraining partial differential equation. Therefore, the cost function cannot simply be differentiated with respect to the parameters. However, optimization algorithms for non-linear equations (as the conjugate gradient or the Newton method) rely on the total derivative of the cost function, which can here be rewritten and specified with the help of the Lagrangian formulation as

$$\begin{aligned}\frac{\mathrm{d}\mathcal{J}(\phi(\mathbf{e}))}{\mathrm{d}\mathbf{e}} &= \frac{\mathrm{d}\mathcal{L}(\phi(\mathbf{e}),\, p;\mathbf{e})}{\mathrm{d}\mathbf{e}} + \frac{\mathrm{d}E(\phi(\mathbf{e}),\, p;\mathbf{e})}{\mathrm{d}\mathbf{e}} \\ &= \left\langle \frac{\partial\mathcal{L}(\phi(\mathbf{e}),\, p;\mathbf{e})}{\partial\phi},\, \frac{\mathrm{d}\phi(\mathbf{e})}{\mathrm{d}\mathbf{e}} \right\rangle + \frac{\partial\mathcal{L}(\phi(\mathbf{e}),\, p;\mathbf{e})}{\partial\mathbf{e}},\end{aligned} \tag{3.4}$$

where $\mathrm{d}E/\mathrm{d}\mathbf{e}$ vanishes since $\phi(\mathbf{e})$ is considered to remain on the manifold of solutions to the weak formulation. This formal calculation of the total derivative of the cost function splits the problem of finding the total derivative of the cost function up into two parts, corresponding to the two terms in the last sum.

(1) The gradient $\nabla_{\mathbf{e}}\phi(\mathbf{e})$ (and therefore, $\mathrm{d}\phi(\mathbf{e})/\mathrm{d}\mathbf{e}$) cannot be calculated, since the solution $\phi(\mathbf{e})$ is not an explicit function of the parameters. This problem can be circumvented if we require that

$$\frac{\partial\mathcal{L}}{\partial\phi} = 0, \tag{3.5}$$

which leads to adjoint equations that restrict the test function p. That idea has been introduced and exploited in previous works by James, Sepulveda and co-workers [38,39,55,56].

(2) Now, given a test function which lets the term $\partial\mathcal{L}/\partial\phi\cdot\mathrm{d}\phi(\mathbf{e})/\mathrm{d}\mathbf{e}$ vanish, the calculation of the total derivative of the cost function reduces to the calculation of the gradient of the Lagrangian with respect to the parameter vector.

3.3. Adjoint state

The adjoint state is given by the requirement (3.5). The conditions on the test function p are obtained after the following straightforward derivation of the derivative of $\mathcal{L}$ taken in the direction of $\delta\phi$:

$$\begin{aligned}&\left\langle \frac{\partial\mathcal{L}}{\partial\phi}(\phi,\, p;\mathbf{e}),\, \delta\phi \right\rangle \\ &\quad= \left\langle \frac{\partial\mathcal{J}(\phi)}{\partial\phi} - \frac{\partial E(\phi,\, p;\mathbf{e})}{\partial\phi},\, \delta\phi \right\rangle \\ &\quad= \iint_{Q_T} \delta\phi(r,t)(\phi(r,t) - \hat{\phi}(r,t))\delta_{\hat{Q}}(r,t)\,\mathrm{d}t\,\mathrm{d}r \\ &\qquad+ \iint_{Q_T} \delta\phi \left(\frac{\partial p}{\partial t} + \partial_\phi f(\phi,r)\frac{\partial p}{\partial r} \right. \\ &\qquad\left. + a(\phi)\frac{\partial^2 p}{\partial r^2} + \partial_\phi s(\phi,r)p \right) \mathrm{d}t\,\mathrm{d}r - \int_{R_0}^{R} \delta\phi(r,T)p(r,T)\,\mathrm{d}r \\ &\qquad+ \int_0^T \delta\phi a(\phi) \left(\frac{\partial p}{\partial r} - \sigma\frac{p}{r} \right)\Bigg|_{r=R_0}^{R} \mathrm{d}t.\end{aligned}$$

The test function p has to be determined in such a way that this quantity vanishes, which leads to the adjoint equation

$$\begin{aligned}&\frac{\partial p}{\partial t} + \partial_\phi f(\phi,r)\frac{\partial p}{\partial r} + a(\phi)\frac{\partial^2 p}{\partial r^2} \\ &\quad= -(\phi - \hat{\phi})\delta_{\hat{Q}}(r,t) - \partial_\phi s(\phi,r)p\end{aligned} \tag{3.6}$$

for $(r,\, t) \in Q_T$, which is a conservation equation for the unknown function p that arises as a backward problem with the end and boundary conditions

$$p(r,T) = 0 \quad \text{for } r \in [R_0,\, R], \tag{3.7}$$

$$\left(\frac{\partial p}{\partial r} - \sigma\frac{p}{r_\mathrm{b}} \right)(r_\mathrm{b}, t) = 0 \quad \text{for } t < T,\, r_\mathrm{b} \in \{R_0,\, R\}. \tag{3.8}$$

The adjoint problem is ill-posed since its solution is not unique: different initial settings could lead to the same prescribed end state.

3.4. Gradient of cost function

Under the condition that the test function p satisfies the adjoint equations and noting that the cost function $\mathcal{J}(\phi(\mathbf{e}))$ is not a function of the parameter vector $\mathbf{e}$ (thus the gradient $\nabla_{\mathbf{e}}\mathcal{J}(\phi(\mathbf{e}))$ vanishes), the total derivative of the cost function is given by

$$\begin{aligned}\frac{\mathrm{d}\mathcal{J}(\phi(\mathbf{e}))}{\mathrm{d}\mathbf{e}} = \iint_{Q_T} &\left(\frac{\mathrm{d}f(\phi,r)}{\mathrm{d}\mathbf{e}}\frac{\partial p}{\partial r} + \frac{\mathrm{d}A(\phi,r)}{\mathrm{d}\mathbf{e}}\frac{\partial^2 p}{\partial r^2} \right. \\ &\left. + \frac{\mathrm{d}s(\phi,r)}{\mathrm{d}\mathbf{e}}p \right) \mathrm{d}t\,\mathrm{d}r,\end{aligned} \tag{3.9}$$

which can be used to employ any gradient algorithm in order to minimize the cost function.

4. Optimization scheme for identification

4.1.1. Discretization of the direct problem

We introduce a standard rectangular grid on Q_T by choosing J, $N \in \mathbb{N}$ and setting $\Delta r := (R - R_0)/J$, $\Delta t := T/N$, $r_j := R_0 + j\Delta r$ and $t_n := n\Delta t$. The numerical scheme for the solution of the direct problem is written in conservative form as a marching formula for the interior points ("interior scheme").

$$\phi_j^{n+1} = \phi_j^n - \lambda_j(F_{j+1/2}^n(\mathbf{e}) - F_{j-1/2}^n(\mathbf{e})) + \mu_j(\mathcal{A}_{j+1/2}^n(\mathbf{e}) - \mathcal{A}_{j-1/2}^n(\mathbf{e})), \quad j = 1, \ldots, J-1, \tag{4.1}$$

where $\lambda_j = \mu_j := \Delta t/(r_j^\sigma \Delta r)$, supplemented by the initial condition

$$\phi_j^0 = \phi_j^{\text{init}}, \quad j = 0, \ldots, J \tag{4.2}$$

and the following discrete versions of the boundary conditions (2.5):

$$\lambda_0 F_{-1/2}^n(\mathbf{e}) - \mu_0 \mathcal{A}_{-1/2}^n(\mathbf{e}) = 0, \tag{4.3}$$

$$\lambda_J F_{J+1/2}^n(\mathbf{e}) - \mu_J \mathcal{A}_{J+1/2}^n(\mathbf{e}) = 0. \tag{4.4}$$

Inserting (4.3) and (4.4) into the formula for the interior scheme, (4.1), we obtain update formulae for the boundary solution values ϕ_0^n and ϕ_J^n, respectively ("boundary scheme"). The numerical flux

$$F_{j+1/2}^n = F_{j+1/2}^n(\phi_{j-K+1}^n, \ldots, \phi_{j+K}^n, r_{j+1/2})$$

and the numerical diffusion term

$$\mathcal{A}_{j+1/2}^n = \mathcal{A}_{j+1/2}^n(\phi_{j-\bar{K}+1}^n, \ldots, \phi_{j+\bar{K}}^n, r_{j+1/2})$$

are specified in Appendix A.

The discrete versions of the unknown ϕ and the test function p are denoted by ϕ_Δ and p_Δ, and ϕ_j^n and p_j^n are the constant values of ϕ_Δ and p_Δ at $(j\Delta r, n\Delta t)$, $(j,n) \in \hat{Q}_\Delta$, respectively, where $\hat{Q}_\Delta := (0, \ldots, J-1) \times (0, \ldots, N-1)$. The calculus for the discrete formulation is analogous to the formal continuous one and thus will also be presented in an analogous structuring, whereas the formal calculus has focused on the formal motivation, the discrete calculus is focused on an efficient scheme as result.

4.2. Discrete optimization with PDE as constraint

The discrete minimization problem is stated as "minimize $\mathcal{J}_\Delta(\phi_\Delta(\mathbf{e}))$ with respect to $\mathbf{e}$", where

$$\mathcal{J}_\Delta(\phi_\Delta(\mathbf{e})) := \frac{\Delta r \Delta t}{2} \sum_{(j,n) \in \hat{Q}_\Delta} (\phi_j^n(\mathbf{e}) - \hat{\phi}_j^n)^2 \tag{4.5}$$

is the discrete cost function. Here, we assume that the identification points in $\hat{Q}$ are actually grid points and $\hat{Q}_\Delta \subset Q_\Delta$ is the index set associated with $\hat{Q}$.

For a given parameter vector $\mathbf{e}$, we express the fact that ϕ is a solution of the discrete direct problem (4.1)–(4.4) by writing

$$E_\Delta(\phi_\Delta(\mathbf{e}), p_\Delta; \mathbf{e}) = 0, \tag{4.6}$$

which is the constraint to the optimization problem, and where $E(\cdot,\cdot;\cdot)$ is defined by

$$\begin{aligned} E_\Delta(\phi_\Delta, p_\Delta; \mathbf{e}) := \sum_{(j,n) \in Q_\Delta} \{ & \phi_j^n(p_j^n - p_j^{n+1}) \\ & + F_{j+1/2}^n(\mathbf{e})(\lambda_j p_j^{n+1} - \lambda_{j+1} p_{j+1}^{n+1}) \\ & - \mathcal{A}_{j+1/2}^n(\mathbf{e})(\mu_j p_j^{n+1} - \mu_{j+1} p_{j+1}^{n+1})\} \\ & + \sum_{j=0}^{J-1} (\phi_j^N p_j^N - \phi_j^0 p_j^0). \end{aligned} \tag{4.7}$$

This expression is derived by multiplying the scheme for the direct problem, (4.1)–(4.4), with p_j^{n+1}, followed by summation over j and n such that in the final form, the sums are taken over differences of the test function. This imitates the continuous weak form, as is detailed in Appendix of [33]. The constraint (4.6) holds for all discrete test functions p_Δ.

4.3. Discrete Lagrangian formulation

The discrete Lagrangian formulation

$$\mathcal{L}_\Delta(\phi_\Delta, p_\Delta; \mathbf{e}) := \frac{1}{\Delta t \Delta r} \mathcal{J}_\Delta(\phi_\Delta) - E_\Delta(\phi_\Delta, p_\Delta; \mathbf{e}) \tag{4.8}$$

is again used to allow an explicit expression for the total derivative of the cost function

$$\begin{aligned} \frac{\mathrm{d}\mathcal{J}_\Delta(\phi_\Delta)}{\mathrm{d}\mathbf{e}} &= \Delta t\, \Delta r \left[\frac{\mathrm{d}\mathcal{L}_\Delta(\phi_\Delta, p_\Delta; \mathbf{e})}{\mathrm{d}\mathbf{e}} + \frac{\mathrm{d}E_\Delta(\phi_\Delta, p_\Delta; \mathbf{e})}{\mathrm{d}\mathbf{e}} \right] \\ &= \Delta t\, \Delta r \left\langle \frac{\partial \mathcal{L}_\Delta(\phi_\Delta, p_\Delta; \mathbf{e})}{\partial \phi_\Delta}, \frac{\mathrm{d}\phi}{\mathrm{d}\mathbf{e}} \right\rangle \\ &\quad + \Delta t\, \Delta r \frac{\mathrm{d}\mathcal{L}_\Delta(\phi_\Delta, p_\Delta; \mathbf{e})}{\mathrm{d}\mathbf{e}}, \end{aligned}$$

which again splits the problem up into two parts: If firstly, the adjoint equation prescribes the test function p_Δ such that $\partial\mathcal{L}/\partial\phi_\Delta = 0$ and the corresponding term vanishes, then, secondly, the gradient with respect to the parameters of the Lagrangian gives a descent direction of the parameter vector for the algorithm.

4.4. Discrete adjoint state

The identity

$$\frac{\partial \mathcal{L}_\Delta}{\partial \phi_j^n} = \frac{\partial \mathcal{J}_\Delta(\phi_\Delta)}{\partial \phi_j^n} - \frac{\partial E_\Delta(\phi_\Delta, p_\Delta; \mathbf{e})}{\partial \phi_j^n} \tag{4.9}$$

leads to the following adjoint scheme for the discrete test function p_j^n

$$\begin{aligned} p_j^n &= p_j^{n+1} - \sum_{k=-K}^{K-1} \frac{\partial F_{j+k+1/2}^n(\mathbf{e})}{\partial \phi_j^n}(\lambda_{j+k} p_{j+k}^{n+1} - \lambda_{j+k+1} p_{j+k+1}^{n+1}) \\ &\quad + \sum_{\ell=-\bar{K}}^{\bar{K}-1} \frac{\partial \mathcal{A}_{j+\ell+1/2}^n(\mathbf{e})}{\partial \phi_j^n}(\mu_{j+\ell} p_{j+\ell}^{n+1} - m_{j+\ell+1} p_{j+\ell+1}^{n+1}) \\ &\quad - (\phi_j^n(\mathbf{e}) - \hat{\phi}_j^n)\delta_{\hat{\mathcal{Q}}_\Delta}(j,n) \\ &\quad \text{for } j = 0, 1, \ldots, J \text{ and } n = N-1, N-2, \ldots, 0 \end{aligned} \tag{4.10}$$

with the end condition

$$\begin{aligned} &p_j^N = 0 \text{ for } 0 \le j \le \max\{K, \bar{K}\} \\ &\text{and } J - \max\{K, \bar{K}\} + 1 \le j \le J, \end{aligned} \tag{4.11}$$

and we consider the conventional notation

$$F_{k+1/2}^n = \mathcal{A}_{\ell+1/2}^n = 0 \quad \text{for } \ell, k \le 1 \text{ and } \ell, k \ge J.$$

4.5. Discrete gradient of cost function

The discrete gradient of the cost function

$$\begin{aligned} \nabla_{\mathbf{e}} \mathcal{J}_\Delta(\mathbf{e}) &= \Delta r\, \Delta t \nabla_{\mathbf{e}} \mathcal{L}_\Delta(\phi_\Delta(\mathbf{e}), p_\Delta; \mathbf{e}) \\ &= -\Delta r\, \Delta t \nabla_{\mathbf{e}} E_\Delta(\phi_\Delta(\mathbf{e}), p_\Delta; \mathbf{e}) \end{aligned} \tag{4.12}$$

where

$$\begin{aligned} \nabla_{\mathbf{e}} E_\Delta &= \sum_{(j,n) \in \mathcal{Q}_\Delta} \nabla_{\mathbf{e}} F_{j+1/2}^n(\mathbf{e})(\lambda_j p_j^{n+1} - \lambda_j p_j^{n+1}) \\ &\quad - \nabla_{\mathbf{e}} \mathcal{A}_{j+1/2}^n(\mathbf{e})(\mu_j p_j^{n+1} + \mu_{j+1} p_{j+1}^{n+1}) \end{aligned} \tag{4.13}$$

finally gives the steepest descent direction.

Note that the calculus performed up to now is independent of the numerical flux function. Now, it only remains to specify how the derivatives of the numerical flux (as desired in (A.2)) are obtained, i.e. "explicit" expressions for the gradients $\nabla_{\mathbf{e}} F_{j+1/2}^n$ and $\nabla_{\mathbf{e}} \mathcal{A}_{j+1/2}^n$ and, more important, for the partial derivatives $\partial F_{j+k+1/2}^n / \partial \phi_j^n$ for $k = -K, \ldots, K-1$ and $\partial \mathcal{A}_{j+\ell+1/2}^n / \partial \phi_j^n$ for $\ell = -\bar{K}, \ldots, \bar{K} - 1$ need to be derived. These quantities are required in the adjoint scheme (4.10). Explicit expressions for these derivatives are provided in Appendix A.

4.6. The parameter identification algorithm

The discrete calculus can be summarized to give the following parameter identification algorithm. We assume that observation data $\hat{\phi}$ are given on part of a grid with mesh width $(\Delta t, \Delta x)$, and we assume that a start parameter vector $\mathbf{e} = \mathbf{e}^{(k)}$ is given ($k = 0$ when the algorithm is started). To determine an improved parameter vector $\mathbf{e}^{(k+1)}$ proceed as follows:

(1) Solve the direct problem numerically using the numerical scheme (4.1)–(4.4) (or one of its implicit or semi-implicit variants), and using the parameter vector $\mathbf{e} = \mathbf{e}^{(k)}$. This yields a discrete solution $\phi_\Delta = \phi_\Delta(\mathbf{e})$.
(2) Use the solution $\phi_\Delta(\mathbf{e})$ to solve the discrete adjoint problem defined by the adjoint scheme (4.10) and the corresponding end condition (4.11) when the solution to the direct problem (in Step 1) has been calculated by an explicit scheme. If an implicit scheme has been used in Step 1, then also an implicit version of the adjoint scheme has to be used. An example of a suitable implicit adjoint scheme is given in Section 5. The result of Step 2 is a specific discrete test function p_Δ.
(3) Use an explicit formula for the discrete gradient of the cost function, for example the one given by (4.12), (4.13) when Steps 1 and 2 have been handled by explicit schemes, to calculate a discrete gradient $\nabla_{\mathbf{e}} \mathcal{J}_\Delta(\mathbf{e})$ of the cost function.
(4) Use the discrete gradient $\nabla_{\mathbf{e}} \mathcal{J}_\Delta(\mathbf{e})$ to find an improved parameter vector $\mathbf{e}^{(k+1)}$ for example by a conjugate gradient method.
(5) If $\mathbf{e}^{(k+1)}$ is a parameter vector of sufficient quality (for example, when $\|\mathbf{e}^{(k+1)} - \mathbf{e}^{(k)}\|$ is small enough), then stop; otherwise, increase k by one and start again with Step 1.

5. Numerical examples

The numerical examples refer to the batch centrifugation of a suspension whose initial concentration is chosen homogeneously as $\phi_0 = 0.07$ on the domain $r \in [R_0, R] = [0.06\,\text{m}, 0.3\,\text{m}]$; the flux function is chosen in accordance with (2.2), where $u_\infty = 0.0001$ m/s, $C = 5$ and $\phi_{\max} = 0.66$, and the angular velocity u is such that $R\omega^2 = 10{,}000$ g. Additionally, we consider the power law function (2.3) with $\sigma_0 = 5.7$ Pa, $k = 9$ and $\phi_c = 0.1$ for the effective solid stress; and finally, the density $\Delta\varrho = 1660\,\text{kg/m}^3$ and the usual gravitational acceleration $g = 9.81\,\text{m/s}^2$.

In these numerical examples, we consider two kinds of observation data: a profile of concentration at $t = T$ as a function of r, and a solution profile at the fixed position $r = R$ as a function of time. These observations are generated by a numerical simulation of the direct problem with the explicit second-order Engquist–Osher scheme and with the discretization parameters $J = 200$ and N such that the following CFL condition (cf. [43]) holds:

$$\frac{R\omega^2}{g} \max_{\phi \in [0, \phi_{\max}]} |f_{\text{bk}}'(\phi)| \frac{\Delta t}{\Delta r} + 2 \max_{\phi \in [0, \phi_{\max}]} a(\phi) \frac{\Delta t}{(\Delta r)^2} < 1 \tag{5.1}$$

The stability requirement imposed by (5.1) to the explicit scheme implies that we need extremely small values of $\Delta t (\approx (\Delta x)^2)$, which considerably increases computational time. This disadvantage is removed by considering a fully

implicit scheme which is unconditionally stable. Thus, for the identification results presented we consider the following first-order implicit discretization of (3.9):

$$\begin{aligned}\phi_j^{n+1} &= \phi_j^n - \lambda_j(F_{j+1/2}^{n+1}(\mathbf{e}) - F_{j-1/2}^{n+1}(\mathbf{e})) \\ &\quad + \mu_j(\mathcal{A}_{j+1/2}^{n+1}(\mathbf{e}) - \mathcal{A}_{j-1/2}^{n+1}(\mathbf{e})), \qquad \phi_j^0 = \phi_j^{\text{init}}, \\ &\quad \lambda_0 F_{-1/2}^{n+1}(\mathbf{e}) - \mu_0 \mathcal{A}_{-1/2}^{n+1}(\mathbf{e}) = 0, \\ &\quad \lambda_J F_{J+1/2}^{n+1}(\mathbf{e}) - \mu_J \mathcal{A}_{J+1/2}^{n+1}(\mathbf{e}) = 0. \end{aligned} \tag{5.2}$$

For each $n = 0, \ldots, N-1$, we have in (5.2) a non-linear system of size $J \times J$, which is solved using the method of Newton–Raphson.

In all tests we consider $N = J$. The weak formulation $E_\Delta = E_\Delta(\phi_\Delta(\mathbf{e}), p_\Delta; \mathbf{e})$ is given by

$$\begin{aligned} E_\Delta &= \sum_{(j,n)\in Q_\Delta} \{\phi_j^n(p_j^n - p_j^{n+1}) \\ &\quad + F_{j+1/2}^n(\lambda_j p_j^n - \lambda_{j+1} p_{j+1}^n) \\ &\quad - \mathcal{A}_{j+1/2}^n(\mu_j p_j^n - \mu_{j+1} p_{j+1}^n)\} \\ &\quad + \sum_{j=0}^{J} \{(\phi_j^N + \lambda_j(F_{j+1/2}^n - F_{j-1/2}^n) - \mu_j(\mathcal{A}_{j+1/2}^N \\ &\quad - \mathcal{A}_{j-1/2}^N)]p_j^N - [\phi_j^0 + \lambda_j(F_{j+1/2}^0 - F_{j-1/2}^0) \\ &\quad - \mu_j(\mathcal{A}_{j+1/2}^0 - \mathcal{A}_{j-1/2}^0)]p_j^0\}. \end{aligned} \tag{5.3}$$

The adjoint scheme and the gradients which are given below are obtained with the methodology developed in Section 4 (including the Appendix A).

We use the conjugate gradient method in the modified form of Polak and Ribière to minimize the objective function $\mathcal{J}(\phi(\mathbf{e}))$, starting with the initial vector

$$\mathbf{e} = (5.5, 6.5, 9.5, 0.08) \tag{5.4}$$

In order to solve the linear minimization step with the conjugate gradient algorithm we employ Wolfe's linear search algorithm as described in [57].

5.1. Example 1: Profile of concentration at t = T as observation

In this example we consider a rotating tube ($\sigma = 0$) and radial profiles at fixed times $\hat{\phi}(r, T)$ with $T \in \{0.3\,\text{s}, 1.2\,\text{s}\}$ as observation data, such that the cost function is given by

$$\mathcal{J}(\phi) = \frac{1}{2}\int_{R_0}^{R} (\phi(r, T) - \hat{\phi}(r, T))^2 \, \mathrm{d}r. \tag{5.5}$$

Let $P^n := (p_0^n, \ldots, p_J^n)$, and denote, for the implicit calculation of the adjoint scheme, by $\mathbf{A}_n$ the $J \times J$ tridiagonal matrix with entries

$$\begin{aligned} a_{j,j-1}^n &= \lambda_{j-1}\frac{\partial F_{j-1/2}^n}{\partial \phi_j^n} - \mu_{j-1}\frac{\partial \mathcal{A}_{j-1/2}^n}{\partial \phi_j^n}, \quad j = 2, \ldots, J, \\ a_{j,j}^n &= 1 + \lambda_j\left(\frac{\partial F_{j+1/2}^n}{\partial \phi_j^n} - \frac{\partial F_{j-1/2}^n}{\partial \phi_j^n}\right) \\ &\quad - \mu_j\left(\frac{\partial \mathcal{A}_{j+1/2}^n}{\partial \phi_j^n} - \frac{\partial \mathcal{A}_{j-1/2}^n}{\partial \phi_j^n}\right), \quad j = 1, \ldots, J-1, \\ a_{j,j+1}^n &= -\lambda_{j+1}\frac{\partial F_{j+1/2}^n}{\partial \phi_j^n} + \mu_{j+1}\frac{\partial \mathcal{A}_{j+1/2}^n}{\partial \phi_j^n}, \\ j &= 1, \ldots, J-1, \qquad a_{0,0}^n = 1 + \lambda_0\frac{\partial F_{1/2}^n}{\partial \phi_0^n} - \mu_0\frac{\partial \mathcal{A}_{1/2}^n}{\partial \phi_0^n}, \\ a_{J,J}^n &= 1 - \lambda_J\frac{\partial F_{J-1/2}^n}{\partial \phi_J^n} + \mu_J\frac{\partial \mathcal{A}_{J+1/2}^n}{\partial \phi_J^n}. \end{aligned}$$

Then P^n is the solution of the linear implicit adjoint scheme $\mathbf{A}_n P^n = P^{n+1}$ for $n = N-1, \ldots, 0$ with the end condition $p_j^N = (\phi_j^N - \hat{\phi}_j^N)/a_{j,j}^N$ for $j \in \{0, 1, \ldots, J\}$. The gradient of the discrete cost function is given by $\nabla_\mathbf{e}\mathcal{J}_\Delta(\mathbf{e}) = -\Delta r \nabla_\mathbf{e} E_\Delta(\phi_\Delta(\mathbf{e}), p_\Delta; \mathbf{e})$ where the gradient of the discrete weak form with respect to the parameters is evaluated from

$$\begin{aligned} \nabla_\mathbf{e} E_\Delta &= \sum_{(j,n)\in Q_\Delta} \{\nabla_\mathbf{e} F_{j+1/2}^n(\lambda_j p_j^n - \lambda_{j+1} p_{j+1}^n) \\ &\quad - \nabla_\mathbf{e}\mathcal{A}_{j+1/2}^n(\mu_j p_j^n - \mu_{j+1} p_{j+1}^n)\} \\ &\quad + \sum_{j=0}^{M} \{[\lambda_j(\nabla_\mathbf{e} F_{j+1/2}^N - \nabla_\mathbf{e} F_{j-1/2}^N) \\ &\quad - \mu_j(\nabla_\mathbf{e}\mathcal{A}_{j+1/2}^N - \nabla_\mathbf{e}\mathcal{A}_{j-1/2}^0)]p_j^N \\ &\quad - [\lambda_j(\nabla_\mathbf{e}\mathcal{A}_{j+1/2}^0 - \nabla_\mathbf{e}\mathcal{A}_{j-1/2}^0) \\ &\quad - \mu_j(\nabla_\mathbf{e}\mathcal{A}_{j+1/2}^0 - \nabla_\mathbf{e}\mathcal{A}_{j-1/2}^0)]p_j^0\}. \end{aligned} \tag{5.6}$$

The identified parameters are shown in Table 1 and the profiles for the two different observation times are presented in Fig. 2. These figures present the results with several step sizes of resolution and thus show the convergence of the numerical identification scheme when the accuracy increases.

Table 1
Example 1: the identified parameters for the observation profiles at $T = 0.3$, 1.2

J	T	C	σ_0	k	ϕ_c
100	0.3	5.500066	6.499970	9.499746	0.109268
	1.2	5.500434	6.499983	9.499801	0.110288
150	0.3	5.499963	6.499959	9.499700	0.108991
	1.2	5.500173	6.499975	9.499766	0.109467
200	0.3	5.500081	6.499966	9.499729	0.108849
	1.2	5.500364	6.499981	9.499813	0.109645

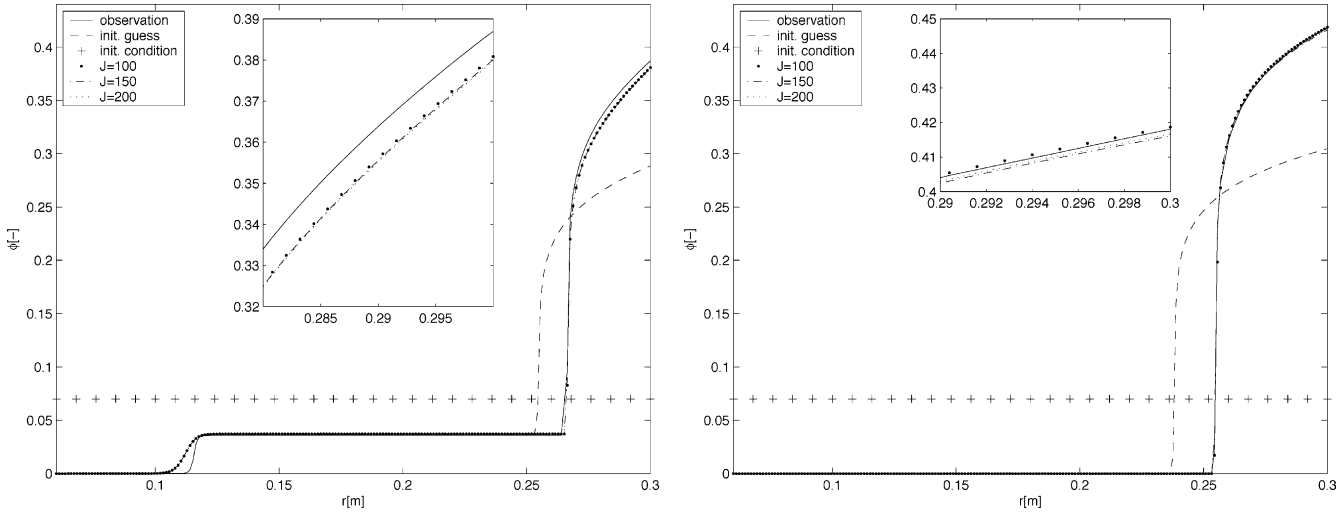

Fig. 2. Example 1: comparison of the observed and identified profiles at $T = 0.3$ (left) and $T = 1.2$ (right).

5.2. *Example 2: Profile of concentration at $z = \bar{R} \in [R_0, R]$ as observation*

In the second example, we consider a cylindrical centrifuge ($\sigma = 1$) and assume that a profile $\phi(\bar{R}, t)$ with $t \in [0, 1.2]$ and $\bar{R} = 0.286$ m is observed, that is, concentrations are measured at a fixed (radial) location as a function of time. This leads to the cost function

$$\mathcal{J}(\phi) = \frac{1}{2} \int_0^T \left(\phi(\bar{R}, t) - \hat{\phi}(\bar{R}, t)\right)^2 \mathrm{d}t. \tag{5.7}$$

In this case, the adjoint scheme is given by $\mathbf{A}_n P^n = P^{n+1} + c$ for $n = N-1, \ldots, 0$ with the end condition $p_j^N = 0$, and where the column vector $\mathbf{c} = (c_1, \ldots, c_J)^T$ is given by

$$c_j = \begin{cases} \phi_j^n - \phi_j^n & \text{if } \bar{R} \in [r_{j-1/2}, r_{j+1/2}], \\ 0 & \text{otherwise,} \end{cases} \qquad j = 1, \ldots, J.$$

The gradient is calculated from $\nabla_{\mathbf{e}} \mathcal{J}_\Delta(\mathbf{e}) = \Delta t \nabla_{\mathbf{e}} E_\Delta \phi_\Delta(\mathbf{e}, p_\Delta; \mathbf{e})$, where $\nabla_{\mathbf{e}} E_\Delta$ is given by (5.6).

The numerically identified parameters, starting from (5.4), are shown in Table 2 and the profiles are given in Fig. 3.

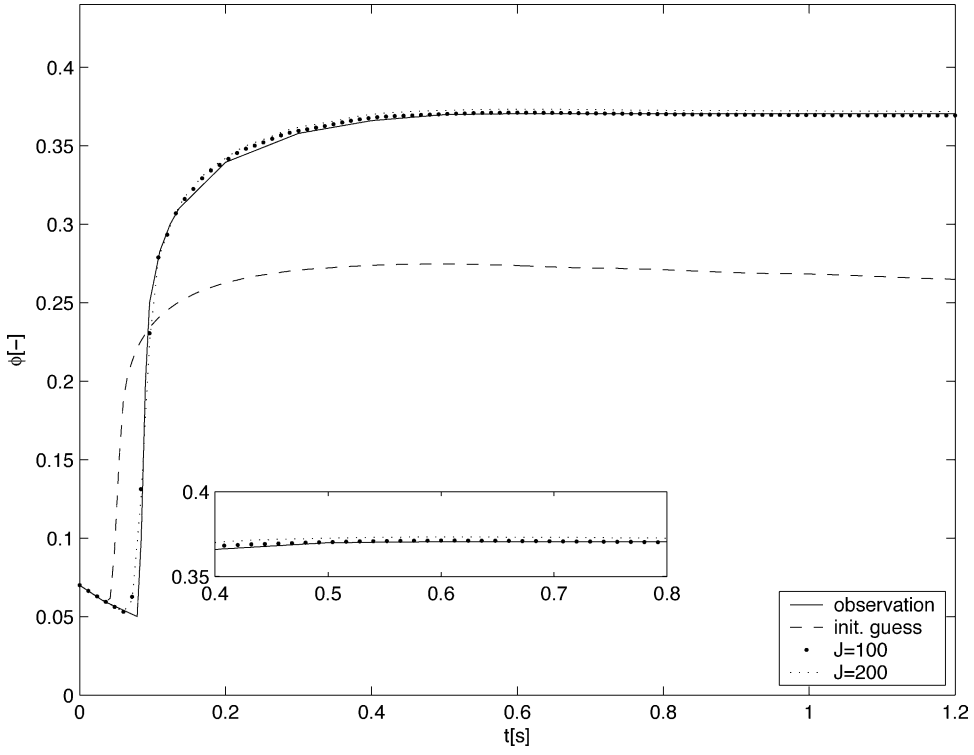

Fig. 3. Example 2: comparison of the observed and identified profiles at the boundary $r = R = 0.3$ with temporal resolution $\Delta t = 0.012$.

Table 2
Example 2: the identified parameters for the observation profile $\hat{R} = R = 0.3$

J	C	σ_0	k	ϕ_c
100	5.500140	6.499936	9.499538	0.109727
200	5.500043	6.499962	9.499705	0.110450

6. Conclusions

This paper has demonstrated that the calculus of inverse problems, which at first seems quite technical, helps to solve one of the fundamental problems in particle technology and, in particular, solid–liquid separation, namely the identification of rheological model functions. The parameter identification framework outlined herein is flexible enough to handle both tube and basket centrifuges (as well as gravity settling systems, which are treated in [34]) in conjunction with: (a) radial concentration profiles measured at a discrete number of times, (b) temporal concentration profiles measured at a fixed radial position, and (c) full measurements of concentrations as functions of position and time, where the positions and times assume values from whole intervals. Measurements leading to data of type (c) are at present technically unconceivable for rotating systems, but can be obtained easily for gravity settling in resting columns [34]. It should be pointed out, however, that accurate concentration measurements of type (a) for rotating tubes and using light extinction are reported in [27,29,32], while type (b) measurements of concentration at a fixed radial position in a basket-type plate-like centrifuge by the method of suctioning probes are reported in [58]. Although, the latter method probably requires a larger total time interval (that is, a low-to-moderate angular velocity), these references illustrate that it is realistic to assume that the measured data used in Examples 1 and 2 are indeed available.

Finally, we should comment on the quality of the parameter identification in these examples, which more precisely present problems of parameter recognition. One would expect that the scheme accurately reproduces the parameters that have actually been used for the simulation. However, we observe in Tables 1 and 2 that the identification moves away very little from the initial guess values of C, σ_0 and k specified by (5.4), while there are considerable changes in the ϕ_c component, namely from 0.08 to values around 0.11, where as the value that is actually used is 0.10. It is however, wrong to presume that the method is flawed, since Figs. 2 and 3 clearly illustrate that the profiles calculated using the parameters identified by our numerical method approximate well the observed data. Rather, these examples seem to alert to the ill-posedness of the problem, which means that the solution to the identification problem in general fails to be unique, and therefore the method may converge to a solution that is not the intend one. Moreover, it appears that the solution profiles of the direct problem depend very critically on the choice of ϕ_c, and to a lesser degree on the other parameters. This leads to the problem of determining the *sensitivities* of the solution with respect to each of the parameters involved, which remains to be done in future work.

Acknowledgments

We acknowledge support by the Collaborative Research Center (Sonderforschungsbereich) 404 at the University of Stuttgart, by the ALECHILE programme financed by DAAD and CONICYT, and FONDECYT 1030718 and 1050728, and Fondap in Applied Mathematics.

Appendix A. Derivatives of numerical fluxes

The numerical scheme (4.1) is based on the non-conservative form (2.1) of the governing equation. Thus, the numerical fluxes $F^n_{j+1/2}$ approximate the physical flux $f(\phi, r) = -\omega^2 r^{1+\sigma}/f_{bk}(\phi)/g$, and $\mathcal{A}^n_{j+1/2}$ is an approximation of $A := r^\sigma \partial_r A(\sigma)$. Here, we consider the forward finite difference approximation of $\partial_r A$, which gives

$$\mathcal{A}^n_{j+1/2} := \frac{A(\phi^n_{j+1}) - A(\phi^n_j)}{\Delta r} r^\sigma_{j+1/2}. \tag{A.1}$$

We employ the numerical flux function corresponding to the Engquist–Osher generalized upwind scheme [17,43,46] defined by

$$F^{EO}(u, v, r) := f(0, r) + \int_0^u \max\{\partial_s f(s, r), 0\}\, ds + \int_0^v \min\{\partial_s f(s, r), 0\}\, ds. \tag{A.2}$$

In the present application, where the dependence of the numerical flux on the position r is of multiplicative type, and the function $f(\cdot, r)$ has only one single maximum, denoted u_m, the integrals in this definition can be easily evaluated, and leads to the explicit formula

$$F^{EO}(u, v, r) = \begin{cases} f(u, r) & \text{for } u \le u_m,\ v \le u_m, \\ f(u, r) & \\ \quad + f(v, r) & \\ -f(u_m, r) & \text{for } u \le u_m,\ v > u_m, \\ f(u_m, r) & \text{for } u > u_m,\ v \le u_m, \\ f(v, r) & \text{for } u > u_m,\ v > u_m, \end{cases} \tag{A.3}$$

which is used for the evaluation of $F^n_{j+1/2}$ be specified below in (A.5).

We now deal with the differentiation with respect to the parameters. In view of (A.2) and (A.3), the problem of calculating the gradient of the numerical flux $F^n_{j+1/2}$ with respect to the parameters is shifted to the calculation of the gradient of the flux f. In addition, from (A.1) the calculation of $\nabla_{\mathbf{e}} \mathcal{A}^n_{j+1/2}$ is given in terms of $\nabla_{\mathbf{e}} \hat{A}$. In our application, the terms introducing the dependence on r do not depend on the parameters,

i.e. we do not deal with shape optimization. Thus, $\nabla_{\mathbf{e}} F^n_{j+1/2}$ is calculated in terms of $\nabla_{\mathbf{e}} f(\phi, r) = r^{1+\sigma} \nabla_{\mathbf{e}} f_{\mathrm{ck}}(\phi)$, where $f_{\mathrm{ck}}(\phi) = -\omega^2 f_{\mathrm{bk}}(\phi)/g$ and $\nabla_{\mathbf{e}} \mathcal{A}^n_{j+1/2}$ is calculated in terms of $\nabla_{\mathbf{e}}$ by

$$\nabla_{\mathbf{e}} \mathcal{A}^n_{j+1/2} := \frac{r^{\sigma}_{j+1/2}}{\Delta r} (\nabla_{\mathbf{e}} A(\phi^n_{j+1}) - (\nabla_{\mathbf{e}} A(\phi^n_j)).$$

To provide expressions for the derivatives with respect to the unknown, we note that $\bar{K} = 1$ in (A.1), which implies the following local derivatives of $\mathcal{A}^n_{j+1/2}$:

$$\frac{\partial \mathcal{A}^n_{j+1/2}}{\partial \phi^n_j} = -\frac{a(\phi^n_j) r^{\sigma}_{j+1/2}}{\Delta r}$$

and

$$\frac{\partial \mathcal{A}^n_{j+1/2}}{\partial \phi^n_{j+1}} = -\frac{a(\phi^n_{j+1}) r^{\sigma}_{j+1/2}}{\Delta r}.$$

The local derivatives of the numerical fluxes with respect to the solution ϕ^n_j are, for the first-order scheme with $F^n_{j+1/2} = F^{\mathrm{EO}}(\phi^n_j, \phi^n_{j+1}, r^n_{j+1/2})$ (i.e., $K = 1$) and as a consequence of (A.2), given by

$$\frac{\partial F_{j+1/2}}{\partial \phi^n_{j+1}} = \max\left\{ \frac{\partial f(\phi^n_j, r_{j+1/2})}{\partial \phi^n_j}, 0 \right\},$$

$$\frac{\partial F_{j+1/2}}{\partial \phi^n_{j+1}} = \min\left\{ \frac{\partial f(\phi^n_{j+1}, r_{j+1/2})}{\partial \phi^n_{j+1}}, 0 \right\}.$$

On the basis of the numerical flux, a second-order scheme can be constructed with a linear reconstruction of the unknown by the slopes

$$s^n_j = \mathrm{MM}\left(\theta \frac{\phi^n_j - \phi^n_{j-1}}{\Delta r}, \frac{\phi^n_{j+1} - \phi^n_{j-1}}{2\Delta r}, \theta \frac{\phi^n_{j+1} - \phi^n_j}{\Delta r} \right),$$

where the standard minmod function

$$\mathrm{MM}(a, b, c) := \begin{cases} \min\{a, b, c\} & \text{if } a, b, c > 0, \\ \max\{a, b, c\} & \text{if } a, b, c \le 0, \\ 0 & \text{otherwise} \end{cases}$$

is used to ensure the TVD property. In order to facilitate the latter calculus, we introduce the local slopes

$$s^-_j := \theta \frac{\phi^n_j - \phi^n_{j-1}}{\Delta r}, \qquad s^0_j := \frac{\phi^n_{j+1} - \phi^n_{j-1}}{2\Delta r},$$

$$s^+_j := \theta \frac{\phi^n_{j+1} - \phi^n_j}{\Delta r}$$

and the indicator functions

$$\chi^*_j := \begin{cases} 1 & \text{if } s^*_j = \max\{s^-_j, s^0_j, s^+_j\} > 0 \text{ or} \\ & \quad s^*_j = \min\{s^-_j, s^0_j, s^+_j\} \le 0, \\ 0 & \text{otherwise,} \end{cases}$$

which select the active slope such that

$$s^n_j = \mathrm{MM}(s^-_j, s^0_j, s^+_j) = \chi^-_j s^-_j + \chi^0_j s^-_j + \chi^+_j s^+_j.$$

In terms of the reconstructions of the solution at the cell boundaries

$$\phi^{\mathrm{R}}_j := \phi^n_j + \frac{\Delta r}{2} s^n_j, \qquad \phi^{\mathrm{L}}_j := \phi^n_j - \frac{\Delta r}{2} s^n_j, \tag{A.4}$$

the numerical flux for the second-order scheme used in (4.1) is based on the evaluation

$$F^n_{j+1/2} = F^{\mathrm{EO}}(\phi^{\mathrm{R}}_j, \phi^{\mathrm{L}}_{j+1}, r_{j+1/2}). \tag{A.5}$$

From (A.4), we see that in this case, $K = 2$. An application of the chain rule shows that the local derivatives of the second order numerical flux are given by

$$\frac{\partial F^n_{j+1/2}}{\partial \phi^n_{j-1}} = \frac{\partial F^n_{j+1/2}}{\partial \phi^{\mathrm{R}}_j} \frac{\partial \phi^{\mathrm{R}}_j}{\partial \phi^n_{j-1}},$$

$$\frac{\partial F^n_{j+1/2}}{\partial \phi^n_j} = \frac{\partial F^n_{j+1/2}}{\partial \phi^{\mathrm{R}}_j} \frac{\partial \phi^{\mathrm{R}}_j}{\partial \phi^n_j} + \frac{\partial F^n_{j+1/2}}{\partial \phi^{\mathrm{L}}_{j+1}} \frac{\partial \phi^{\mathrm{L}}_{j+1}}{\partial \phi^n_j},$$

$$\frac{\partial F^n_{j+1/2}}{\partial \phi^n_{j+1}} = \frac{\partial F^n_{j+1/2}}{\partial \phi^{\mathrm{R}}_j} \frac{\partial \phi^{\mathrm{R}}_j}{\partial \phi^n_{j+1}} + \frac{\partial F^n_{j+1/2}}{\partial \phi^{\mathrm{L}}_{j+1}} \frac{\partial \phi^{\mathrm{L}}_{j+1}}{\partial \phi^n_{j+1}},$$

$$\frac{\partial F^n_{j+1/2}}{\partial \phi^n_{j+2}} = \frac{\partial F^n_{j+1/2}}{\partial \phi^{\mathrm{L}}_{j+1}} \frac{\partial \phi^{\mathrm{L}}_{j+1}}{\partial \phi^n_{j+2}},$$

where

$$\frac{\partial F^n_{j+1/2}}{\partial \phi^{\mathrm{R}}_j} = \max\left\{ \frac{\partial f(\phi^{\mathrm{R}}_j, r_{j+1/2})}{\partial \phi^{\mathrm{R}}_j}, 0 \right\}$$

and

$$\frac{\partial F^n_{j+1/2}}{\partial \phi^{\mathrm{L}}_{j+1}} = \max\left\{ \frac{\partial f(\phi^{\mathrm{L}}_{j+1}, r_{j+1/2})}{\partial \phi^{\mathrm{L}}_{j+1}}, 0 \right\},$$

and where the derivatives of ϕ^{R}_j and ϕ^{L}_{j+1} are evaluated from

$$\frac{\partial \phi^{\mathrm{R}}_j}{\partial \phi^n_{j-1}} = \frac{\Delta r}{2} \frac{\partial s^n_j}{\partial \phi^n_{j-1}}, \qquad \frac{\partial \phi^{\mathrm{R}}_j}{\partial \phi^n_j} = 1 + \frac{\Delta r}{2} \frac{\partial s^n_j}{\partial \phi^n_j},$$

$$\frac{\partial \phi^{\mathrm{R}}_j}{\partial \phi^n_{j+1}} = \frac{\Delta r}{2} \frac{\partial s^n_j}{\partial \phi^n_{j+1}}, \qquad \frac{\partial \phi^{\mathrm{L}}_j}{\partial \phi^n_{j-1}} = -\frac{\Delta r}{2} \frac{\partial s^n_j}{\partial \phi^n_{j-1}},$$

$$\frac{\partial \phi^{\mathrm{L}}_j}{\partial \phi^n_j} = 1 - \frac{\Delta r}{2} \frac{\partial s^n_j}{\partial \phi^n_j}, \qquad \frac{\partial \phi^{\mathrm{L}}_j}{\partial \phi^n_{j+1}} = -\frac{\Delta r}{2} \frac{\partial s^n_j}{\partial \phi^n_{j+1}},$$

which are a consequence of (A.4). The slope derivatives are in turn given by

$$\frac{\partial s^n_j}{\partial \phi^n_{j-1}} = -\frac{\theta}{\Delta r} \chi^-_j - \frac{1}{2\Delta r} \chi^0_j, \qquad \frac{\partial s^n_j}{\partial \phi^n_j} = \frac{\phi}{\Delta r} (\chi^-_j - \chi^+_j),$$

$$\frac{\partial s^n_j}{\partial \phi^n_{j+1}} = \frac{1}{2\Delta r} \chi^0_j + \frac{\theta}{\Delta r} \chi^+_j.$$

References

[1] S. Berres, R. Bürger, K.H. Karlsen, E.M. Tory, Strongly degenerate parabolic-hyperbolic systems modeling polydisperse sedimentation with compression, SIAM J. Appl. Math. 64 (2003) 41–80.

[2] R. Bürger, F. Concha, Mathematical model and numerical simulation of the settling of flocculated suspensions, Int. J. Multiphase Flow 24 (1998) 1005–1023.

[3] R. Bürger, W.L. Wendland, F. Concha, Model equations for gravitational sedimentation-consolidation processes, Z. Angew. Math. Mech. 80 (2000) 79–92.

[4] A.A.A. Aziz, R.G. de Kretser, D.R. Dixon, P.J. Scales, The characterisation of slurry dewatering, Water Sci. Technol. 41 (8) (2000) 9–16.

[5] R.G. de Kretser, S.P. Usher, P.J. Scales, D.V. Boger, K.A. Landman, Rapid filtration measurement of dewatering design and optimization parameters, AIChE J. 47 (2001) 1758–1769.

[6] D.R. Lester, Colloidal suspension dewatering analysis, Ph.D. Thesis, Department of Chemical Engineering, University of Melbourne, Australia, 2002.

[7] S.P. Usher, R.G. De Kretser, P.J. Scales, Validation of a new filtration technique for dewaterability characterization, AIChE J. 47 (2001) 1561–1570.

[8] M.C. Bustos, F. Concha, R. Bürger, E.M. Tory, Sedimentation and Thickening, Kluwer Academic Publishers, Dordrecht, The Netherlands, 1999.

[9] G.J. Kynch, A Theory of Sedimentation, Trans. Farad. Soc. 48 (1952) 166–176.

[10] G. Anestis, Eine eindimensionale Theorie der Sedimentation in Absetzbehältern veränderlichen Querschnitts und in Zentrifugen. Doctoral Thesis, Technical University of Vienna, Austria, 1981.

[11] G. Anestis, W. Schneider, Application of the theory of kinematic waves to the centrifugation of suspensions, Ing.-Arch. 53 (1983) 399–407.

[12] R. Bürger, S. Evje, K.H. Karlsen, On strongly degenerate convection-diffusion problems modelling sedimentation-consolidation processes, J. Math. Anal. Appl. 247 (2000) 517–556.

[13] R. Bürger, K.H. Karlsen, A strongly degenerate convection-diffusion problem modeling centrifugation of flocculated suspensions, in: H. Freistiihler, G. Warnecke (Eds.), Hyperbolic Problems: Theory, Numerics, Applications, vol. I, Birkhauser, Basel, 2001, pp. 207–216.

[14] K.H. Karlsen, M. Ohlberger, A note on the uniqueness of entropy solutions of nonlinear degenerate parabolic equations, J. Math. Anal. Appl. 275 (2002) 439–458.

[15] K.H. Karlsen, N.H. Risebro, On the uniqueness and stability of entropy solutions of nonlinear degenerate parabolic equations with rough coefficients, Discr. Cont. Dyn. Syst. A 9 (2003) 1081–1104.

[16] R. Bürger, S. Evje, K.H. Karlsen, K.-A. Lie, Numerical methods for the simulation of the settling of flocculated suspensions, Chem. Eng. J. 80 (2000) 91–104.

[17] R. Bürger, K.H. Karlsen, On some upwind schemes for the phenomenological sedimentation-consolidation model, J. Eng. Math. 41 (2001) 145–166.

[18] R. Bürger, F. Concha, F.M. Tiller, Applications of the phenomenological theory to several published experimental cases of sedimentation processes, Chem. Eng. J. 80 (2000) 105–117.

[19] P. Garrido, R. Bürger, F. Concha, Settling velocities of particulate systems: 11. Comparison of the phenomenological sedimentation-consolidation model with published experimental results, Int. J. Miner. Process. 60 (2000) 213–227.

[20] P. Garrido, R. Burgos, F. Concha, R. Bürger, Software for the design and simulation of gravity thickeners, Miner. Eng. 16 (2003) 85–92.

[21] P. Garrido, R. Burgos, F. Concha, R. Bürger, Settling velocities of particulate systems: 13. Software for the batch and continuous sedimentation of flocculated suspensions, Int. J. Miner. Process. 73 (2004) 131–144.

[22] C.P. Chu, S.P. Ju, D.J. Lee, K.K. Mohanty, Batch gravitational sedimentation of slurries, J. Colloid Interf. Sci. 245 (2002) 178–186.

[23] C.P. Chu, S.P. Ju, D.J. Lee, F.M. Tiller, K.K. Mohanty, Y.C. Chang, Batch settling of flocculated clayey slurry, Ind. Eng. Chem. Res. 41 (2002) 1227–1233.

[24] C.P. Chu, D.J. Lee, Solids fluxes in consolidating slurries, J. Chin. Inst. Chem. Eng. 32 (2001) 547–554.

[25] C.P. Chu, D.J. Lee, J.H. Tay, Gravitational sedimentation of flocculated waste activated sludge, Water Res. 37 (2003) 155–163.

[26] M.D. Green, K.A. Landman, R.G. de Kretser, D.V. Boger, Pressure filtration technique for complete characterization of consolidating suspensions, Ind. Eng. Chem. Res. 37 (1998) 4152–4156.

[27] S. Berres, R. Bürger, D. Lerche, Identification of particle size distribution based on transmission profiles measured by photocentrifuges, Congress Program and Abstracts, p. 20.6 (abstract, full-length contribution published on CD-ROM), in: S.E. Pratsinis, H. Schulz, R. Strobel, C. Schreglmann (Eds.), PARTEC 2004 International Congress for Particle Technology, Nuremberg, March 16-18, 2004.

[28] C.P. Chu, D.J. Lee, Experimental analysis of centrifugal dewatering process of polyelectrolyte flocculated waste activated sludge, Water Res. 35 (2001) 2377–2384.

[29] D. Frömer, D. Lerche, An experimental approach to the study of the sedimentation of dispersed particles in a centrifugal field, Arch. Appl. Mech. 72 (2002) 85–95.

[30] K.J. Hwang, W.T. Chu, W.M. Li, A method to determine the cake properties in centrifugal dewatering, Sep. Sci. Technol. 36 (2001) 2693–2706.

[31] D. Lerche, Dispersion stability and particle characterization by sedimentation kinetics in a centrifugal field, J. Disp. Sci. Technol. 23 (2002) 699–709.

[32] D. Lerche, D. Fromer, Theoretical and experimental analysis of the sedimentation kinetics of concentrated red cell suspensions in a centrifugal field: determination of the aggregation and deformation of RBC by flux density and viscosity functions, Biorheology 38 (2001) 249–262.

[33] S. Berres, R. Bürger, A. Coronel, M. Sepúlveda, Numerical identification of parameters for a strongly degenerate convection-diffusion problem modelling centrifugation of flocculated suspensions, Appl. Numer. Math. 52 (2005) 311–337.

[34] A. Coronel, F. James, M. Sepúlveda, Numerical identification of parameters for a model of sedimentation processes, Inv. Prob. 19 (2003) 951–972.

[35] J.R. Cannon, Determination of certain parameters in heat conduction problems, J. Math. Anal. Appl. 8 (1964) 188–201.

[36] J.R. Cannon, D. Zachmann, Parameter determination in parabolic partial differential equations from overspecified boundary data, Int. J. Eng. Sci. 20 (1982) 779–788.

[37] S. Gutman, Identification of discontinuous parameters in flow equations, SIAM J. Control Optim. 28 (1990) 1049–1060.

[38] F. James, M. Sepúlveda, Parameter identification for a model of chromatographic column, Inv. Prob. 10 (1994) 1299–1314.

[39] F. James, M. Sepúlveda, Convergence results for the flux identification in a scalar conservation law, SIAM J. Control Optim. 37 (1999) 869–891.

[40] Y.L. Keung, Y. Zou, Numerical identification of parameters in parabolic systems, Inv. Prob. 14 (1998) 83–100.

[41] K. Kunisch, L. White, The parameter estimation problem for parabolic equations and discontinuous observation operators, SIAM J. Control Optim. 23 (1985) 900–927.

[42] M. Yamamoto, Y. Zou, Simultaneous reconstruction of the initial temperature and heat radiative coefficient, Inv. Prob. 17 (2001) 1181–1202.

[43] R. Bürger, F. Concha, Settling velocities of particulate systems: 12. Batch centrifugation of flocculated suspensions, Int. J. Miner. Process. 63 (2001) 115–145.

[44] B. Cockburn, G. Gripenberg, Continuous dependence on the nonlinearities of solutions of degenerate parabolic equations, J. Diff. Eqns. 151 (1999) 231–251.
[45] S. Evje, K.H. Karlsen, N.H. Risebro, A continuous dependence result for nonlinear degenerate parabolic equations with spatially dependent flux function, in: H. Freistühler, G. Warnecke (Eds.), Hyperbolic Problems: Theory, Numerics, Applications, vol. I, Birkhauser, Basel, 2001, pp. 337–346.
[46] B. Engquist, S. Osher, One-sided difference approximations for nonlinear conservation laws, Math. Comp. 36 (1981) 321–351.
[47] R.M. Lueptow, W. Hiibler, Sedimentation of a suspension in a centrifugal field, J. Biomech. Eng. 113 (1991) 485–491.
[48] M. Ungarish, On the separation of a suspension in a tube centrifuge, Int. J. Multiphase Flow 27 (2001) 1285–1291.
[49] J.F. Richardson, W.N. Zaki, Sedimentation and fluidization: Part I, Trans. Inst. Chem. Eng. (London) 32 (1954) 35–53.
[50] F.M. Tiller, W.F. Leu, Basic data fitting in filtration, J. Chin. Inst. Chem. Eng. 11 (1980) 61–70.
[51] R. Bürger, F. Concha, P. Garrido, A unified mathematical model of thickening, filtration and centrifugation of flocculated suspensions, in: A.B. da Luz, P.S.M. Soares, M.L. Torem, R.B.E. Trindade (Eds.), Proceedings of the VI Southern Hemisphere Meeting on Mineral Technology, Rio de Janeiro, Brazil, May 27–31, vol. 1, CETEM/MCT, 2001, pp. 123–129.
[52] P. Garrido, F. Concha, R. Bürger, Application of the unified model of solid-liquid separation of flocculated suspensions to experimental results, in: A.B. da Luz, P.S.M. Soares, M.L. Torem, R.B.E. Trindade (Eds.), Proceedings of the VI Southern Hemisphere Meeting on Mineral Technology, Rio de Janeiro, Brazil, May 27-31, vol. 1, CETEM/MCT, 2001, pp. 117–122.
[53] P. Garrido, F. Concha, R. Bürger, Settling velocities of particulate systems: 14. Unified model of sedimentation, centrifugation and filtration of flocculated suspensions, Int. J. Miner. Process. 72 (2003) 57–74.
[54] S. Berres, R. Bürger, On gravity and centrifugal settling of polydisperse suspensions forming compressible sediments, Int. J. Solids Struct. 40 (2003) 4965–4987.
[55] G. Guiochon, F. James, M. Sepúlveda, Numerical results for the flux identification in a system of conservation laws, in: M. Fey, R. Jeltsch (Eds.), Hyperbolic Problems: Theory, Numerics, Applications, vol. I, Birkhäuser, Basel, 1999, pp. 423–432.
[56] F. James, M. Postel, M. Sepúlveda, Numerical comparison between relaxation and nonlinear equilibrium models. Application to chemical engineering, Phys. D 138 (2000) 316–333.
[57] J.-B. Hiriart-Urruty, C. Lemaréchal, Convex Analysis and Minimization Algorithms I, Springer-Verlag, Berlin, 1993.
[58] J. Dueck, D.Y. Kilimnik, L.I. Minkov, T. Neeße, Measurements of the rate of sedimentation of fine particles in a platelike centrifuge, J. Eng. Phys. Thermophys. 76 (2003) 748–759.